Friction Stir Welding of Al 2024 with Al 7075 Alloys and evaluate its structural and mechanical properties

S.Z.Anvari [1,*], S. Rohani Mojarad[2]

[1] *Department of Mechanical Engineering, Payame Noor University (PNU), P.O. Box, 19395-3697, Tehran, Iran*
[2] *Department of Mechanical Engineering, Daneshpajoohan Institute of Higher Education, Isfahan, Iran.*

ARTICLE INFO

Article history:

Received 19 June 2018
Accepted 6 November 2018
Available online 1 December 2018

Keywords:

Friction stir welding
Aluminum alloys
Al2024
Al7075

ABSTRACT

The overarching goal of this research was to use the FSW method to join the Al 2024 and Al 7075 alloys, examine the structural and mechanical properties of the joint, and eventually find the optimum welding parameters. The welding operation was carried out using a milling machine and a device with cylindrical pins. The transverse cross-section of the weld was used for optical as well as electron microscopy observations. The evaluation of mechanical properties at room temperature, i.e., tensile strength and hardness were done. The size of the grains measured using an optical microscope varied between approximately 2.6 and 11 μm. The results of the welding process revealed that the specimen with a traverse speed of 30 mm/min, a rotation speed of 600 rpm, and the highest ultimate tensile strength (195 MPa), and the specimen with a traverse speed of 70 mm/min, a rotation speed of 1200 rpm, and an ultimate tensile strength of 193 MPa were selected as the optimum specimens due to their off-fusion-zone failure, their high strength in the tensile strength test, and their adequate input heat. Moreover, in the specimen with the traverse speed of 100 mm/min and the rotation speed of 600 rpm, the highest percentage of elongation (3.80%) was observed in the tensile strength test. The results from the tensile test indicated that with a decrease in the traverse speed, the tensile strength of the specimens increased, the elongation percent decreased, and the stirring improved.

1-Introduction

Aluminum has numerous applications in industries such as the automotive, military, and aerospace industries. This metal is extremely light-weight and some of its alloys are stronger than the structural steel. Among the various alloys of aluminum, the 2XXX and 7XXX series are used for military purposes due to their high strength [1]. Moreover, of the 2XXX and 7XXX series alloys, the 2024 and 7075 alloys are used in the structures because of their high strength [2-4].

The alloys of the 2XXX and 7XXX series are generally classified as non-weldable because of poor solidification microstructure and porosity in the fusion zone. Moreover, given the weak microscopic structure and the pores in the FZ zone, the properties of the fusion zone are not comparable to the base metal [5]. As a result of these factors, the Welding Institute (TWI) of Cambridge (England) invented the friction stir welding (FSW) method in 1991 for welding the aluminum alloys that could not be welded using the conventional welding methods [6, 7]. The

* Corresponding author:
E-mail address: szaanvari@gmail.com

friction stir welding (FSW) method is a solid-state method with advantages such as high energy efficiency and environment-friendliness. This method is also used in the aerospace industry and other critical industries to join the high-strength base aluminum alloys that cannot be easily welded using the conventional methods. Today, this method is extensively used to join various materials, especially the heterogeneous metals and aluminum alloys [8]. This method not only does not suffer the limitations of the fusion welding method, but also does offer numerous advantages such as the possibility of dissimilar metals with different melting points and high strengths. Among the reasons for using this method are the problems about the fusion welding of the aluminum alloys. The susceptibility of the 2024 and 7075 alloys to hot cracking is caused by the wide range of the solidification zone in the presence of more alloy elements. Besides, given the high tendency of the molten aluminum to join oxygen, aluminum oxide rapidly forms during the fusion welding processes and the melting does not occur completely due to the higher melting point of the aluminum oxide as compared to pure aluminum. If the resulting oxides do not form an adequately thick layer, they will prevent the formation of arcs at the beginning of the welding process due to their function as electrical insulators. On the other hand, the thermal expansion coefficient of the aluminum alloys is large and twice that of steel. Therefore, the welding fittings rapidly cool down after reaching the melting temperature and display a considerable residual stress. Even by using the shielding gases or fluxes in the 2024 and 7075 alloys it is not possible to easily obtain a fitting. Hence, it is necessary to investigate new methods of solid-state welding including the FSW method to overcome the mentioned problems, improve quality, and accelerate the welding process.

The difficulty of obtaining high-strength welds, which are resistant to fatigue and failure, using the fusion welding methods and the aluminum alloys used in the aerospace industry has reduced the applications of the 2024 and 7075 alloys. These alloys are generally classified as non-weldable alloys. In addition, the decline of the mechanical properties of welds as compared to the base metals is dramatic in these alloys. As a result of these problems, it is unacceptable to join these alloys using the common welding methods [9-11]. Goloborodko et al. [12] reported that FSW of 7075-T6 aluminum alloy results in the formation of a homogeneous fine grained structure with an average size of about 3 mm.

In the FSW process, a tool with a special shape and a high rotation speed is placed in the joint, and as a result of the rotation of the tool, the frictional heat required for the joining process is produced. The movement of the rotary tool fills the joint and facilitates the joining process [13, 14]. In the process of joining the aluminum alloys using the FSW method, many parameters such as the rotation speed, traverse speed, shape, and geometry of the tools influence the microstructural and mechanical properties of the joint [15].

The present research objectives were to join the 2024 and 7075 alloys of aluminum with a thickness of 3mm at four traverse speeds and four rotation speeds and also study the structural and mechanical properties of these alloys using the friction stir welding (FSW) method. The ultimate goal of this research was to find the optimum parameters considering the mechanical and microstructural properties. After conducting an FSW welding operation, a number of studies on the microstructural properties of the fusion zone were carried out using the microscopic and macroscopic methods. The onion rings were also examined, the SEM (scanning electron microscope) images were analyzed, and the results were classified properly.

2. Experimental

In this research, the 2024-T4 and 7075-T6 aluminum alloys were used in the form of sheets with a thickness of 3mm, a width of 50mm, and a length of 100mm for butt welding. The standard chemical composition [16] and Experimental chemical composition of the aluminum alloys are listed in Tables 1 and 2. A milling machine was used to perform the welding and joining operations. In the welding process, the parts were fixed using fixtures due to the existence of extremely large forces. During this process, the edges of the sheets must be completely tangent without any space between them. Therefore, the second sheet was tangent to the first sheet, and the sheets were fixed using fixtures. The tool used in this process

was made of H13 hot-work steel in the form of a cylinder without screw threads. The overall length of the tool, the pin length, the pin diameter, and the shoulder diameter (or weld width) were 100mm, 2.7mm, 6mm, and 18mm, respectively (Fig. 1). Fig. 2 also depicts a top view of the FSW weld. The sheets were welded at four different rotation and traverse speeds as indicated in Table 3. These diverse speeds were selected to find the optimum values, which refer to the lack of any defect in the visual tests.

Table 1. Chemical composition of Al 2024.

Element (wt. %)	Cu	Si	Mg	Fe	Mn	Cr	Zn	Ti	Al
Standard chemical composition	3.5-4.5	0.9	0.9-0.45	0.5	0.2	0.1	0.25	0.15	Bal.
Experimental chemical composition	4.2	0.224	0.4	0.05	0.17	0.008	0.15	0.026	92.05

Table 2. Chemical composition of Al 7075.

Element (wt. %)	Zn	Mg	Cu	Si	Fe	Mn	Cr	Ti	Al
Standard chemical composition	5.1-6.1	2.1-2.9	1.2-2	0.4	0.5	0.3	0.18-0.28	0.2	Bal.
Experimental chemical composition	5.63	2.4	1.67	0.06	0.1	0.08	0.2	0.035	89.78

Fig. 1. Dimensions of the tool designed for friction stir welding.

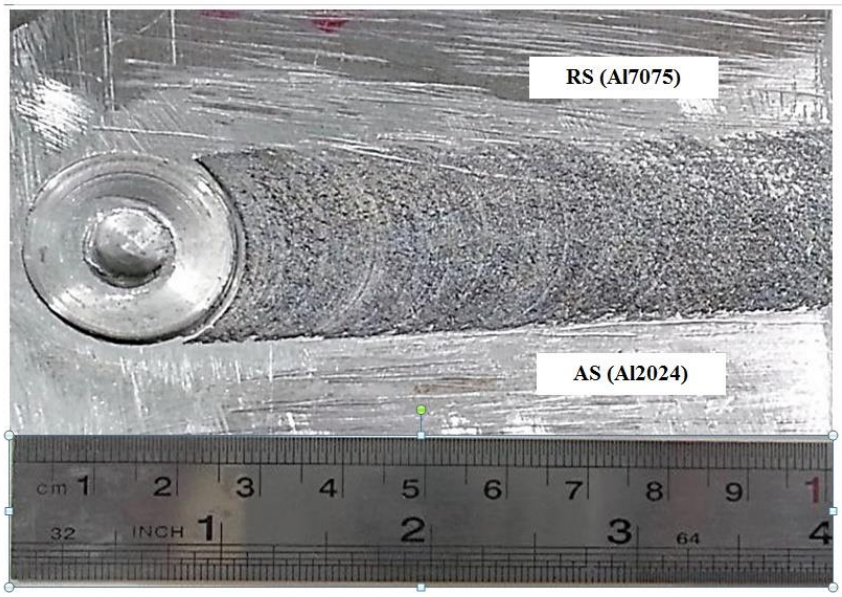

Fig. 2. A top view of the FSW weld.

Table 3. Experimental parameters set up.

Weld number	Rotational speed (r/min)	Travel speed (mm/min)
FSW-01	1200	100
FSW-02	1200	70
FSW-03	1200	50
FSW-04	800	50
FSW-05	800	30
FSW-06	800	100
FSW-07	600	30
FSW-08	600	100
FSW-09	1000	50
FSW-10	1000	100

The specimens were cut by a wire cutting machine and all welds were examined for their shapes and macroscopic properties to ensure the lack of apparent defects such as cracks and holes. After cutting the specimens, the tensile strength test was conducted. The tensile strength test was carried out in accordance with the ASTM E8 using a tensile tester with a jaw speed of 2mm/min and a maximum capacity of 2 tons. Fig. 3 shows testing specimens.

Following the welding process, the metallography testing of the specimens was conducted using an optical microscope for the microscopic studies, onion ring analyses, and SEM analyses. To this end, the cross sections of the specimens were ground. Afterwards, the specimens were polished and were etched using a Keller solution.

The micro-hardness test was also performed within 10 seconds in terms of Vickers hardness using a hardness tester with a load of 200 grams. The diagram of the hardness profile of the specimens was also drawn.

Finally, the optimum specimens were selected and the results were properly classified based on the results of the tensile strength test and parameters such as the mechanical properties, the off-fusion-zone failure in the tensile test, and the improved microstructure.

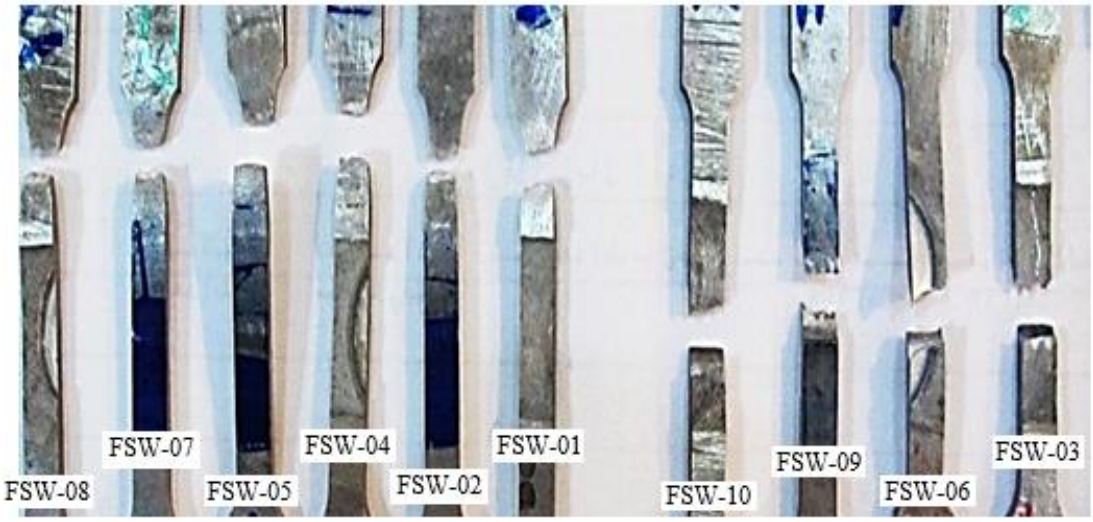

Fig. 3.Testing specimens.

3. Results and discussion

The tensile strength test was carried out to find the optimum specimens. Fig. 4 and 5 show the stress-strain curves of weld FSW-02 and FSW-07. The results of the tensile tests conducted on the specimens are shown in Fig. 6 and Table 4. According to these results, the traverse speed decreases, the elongation decreases and the ultimate tensile strength increases at a constant rotation speed. Moreover, with an increase in the traverse speed at a constant rotation speed, the elongation increases similar to the results reported by researchers [17]. Specimens FSW-02 (1200rpm, 70mm/min) and FSW-07 (600rpm, 30mm/min) have the highest tensile strength and off-fusion-zone failure (in the 2024 alloy section).

Afterwards, specimens FSW-01, FSW-02, FSW-04, FSW-05, FSW-07 and FSW-08 were selected as the welding-compatible samples based on the conditions listed in Table 4 and specimens FSW-03, FSW-06, FSW-09 and FSW-10 were not selected as the samples suitable for welding due to their fusion zone failure. Therefore, the latter specimens were excluded from the optimum state specimens group. These six specimens were selected due to their off-fusion-zone failure, which was indicative of the extremely high quality of the welds and their higher strength as compared to the other specimens except for specimen FSW-03. In fact, welds should not yield to failure in the fusion zone during the tensile strength test, and the reason for the higher strength of these specimens was their off-fusion-zone failure. In the optimum welding states, the failure occurred in the alloy precursor (AS) or the 2024 aluminum alloy, which showed a lower tensile strength. In general, tensile strength is deeply dependent on the weld quality and the absence of defects in the fusion zone. Defects and minimum hardness are the main two factors that determine the failure zone. In the defect-free specimens, the zone with the minimum hardness is the cause of failure. The failure in the FSW butt welds in the tensile strength test normally occurs in the zones with the minimum hardness. In the defective welds, the failure zone is determined by the following two factors: 1) the concentration of stress on the defect zone; 2) the distribution of hardness across the fusion zone (FZ) [18]. In this research, due to the presence of zones with more tension around the alloy precursor or the 2024 alloy, either the concentrated stress or the lower ultimate tensile strength (depending on the tensile strength of the base metals in Table 5) could be considered the cause of failure.

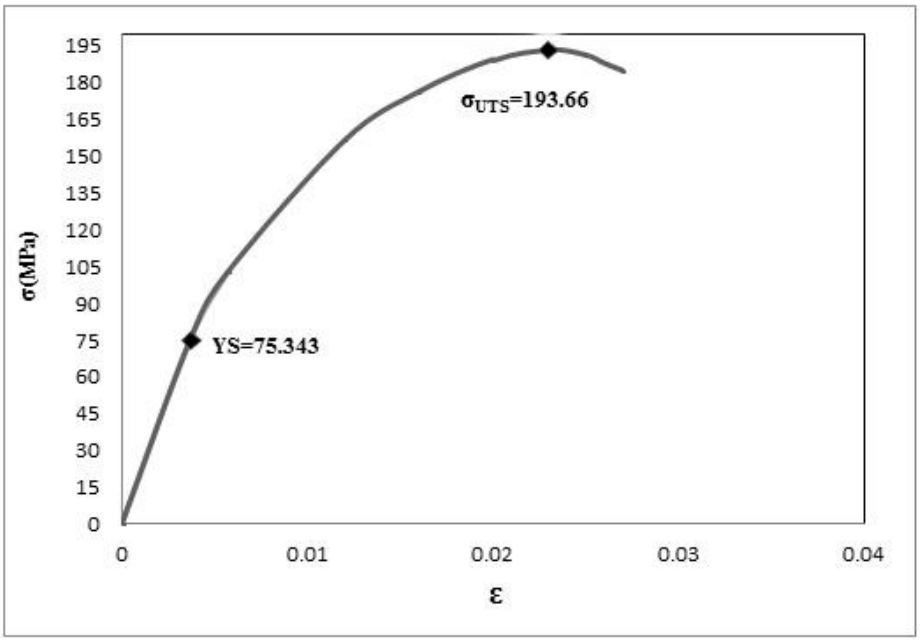

Fig.4. Stress – Strain curve of weld FSW-02.

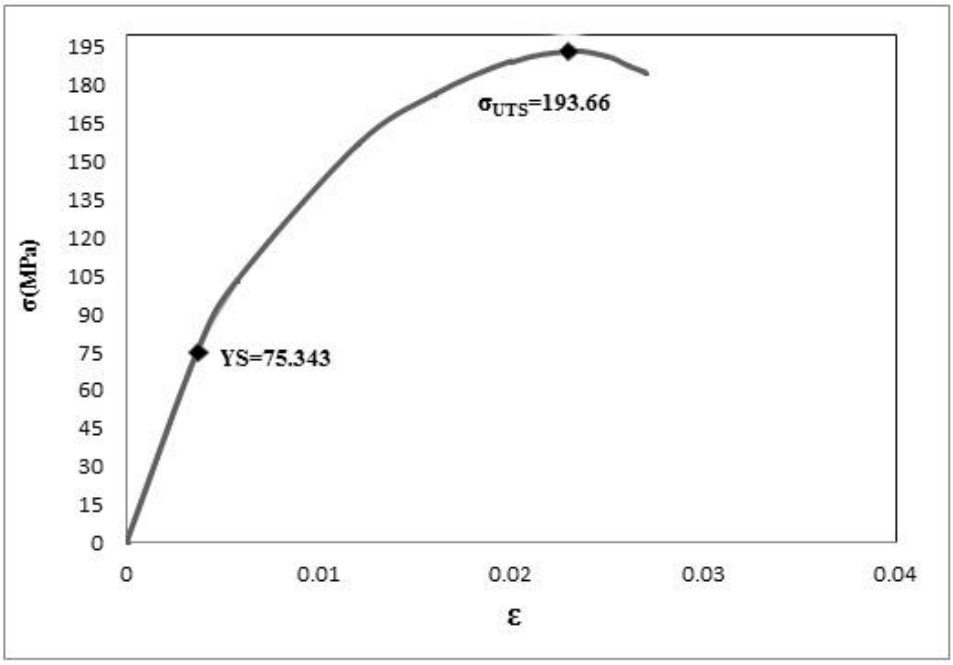

Fig.5. Stress – Strain curve of weld FSW-07.

Table 4. Results of tensile and hardness tests.

Weld Number	Rotation speed (rpm)	Traverse speed (mm/min)	Max load(N)	σ_{UTS} (MPa)	Yield strength (MPa)	Elongation (%)	Grain size (μm)	Hardness (HV)	Rotation speed/ Traverse speed (r/mm)
FSW-01	1200	100	3691	164	72	3.7	---		12
FSW-02	1200	70	3764	193	75	2.3	2.6		17
FSW-03	1200	50	5286	271	144	2.7	8.5	136±1.2	24
FSW-04	800	50	3647	186	73	2.8	---	138±1.2	16
FSW-05	800	30	3652	188	99	2.0	---		26
FSW-06	800	100	3543	189	136	3.1	6.5		8
FSW-07	600	30	3817	195	88	1.7	---		20
FSW-08	600	100	3548	175	112	3.8	---		6
FSW-09	1000	50	3364	172	103	1.8	11	131±1.8	20
FSW-10	1000	100	3113	160	74	1.8	---		10

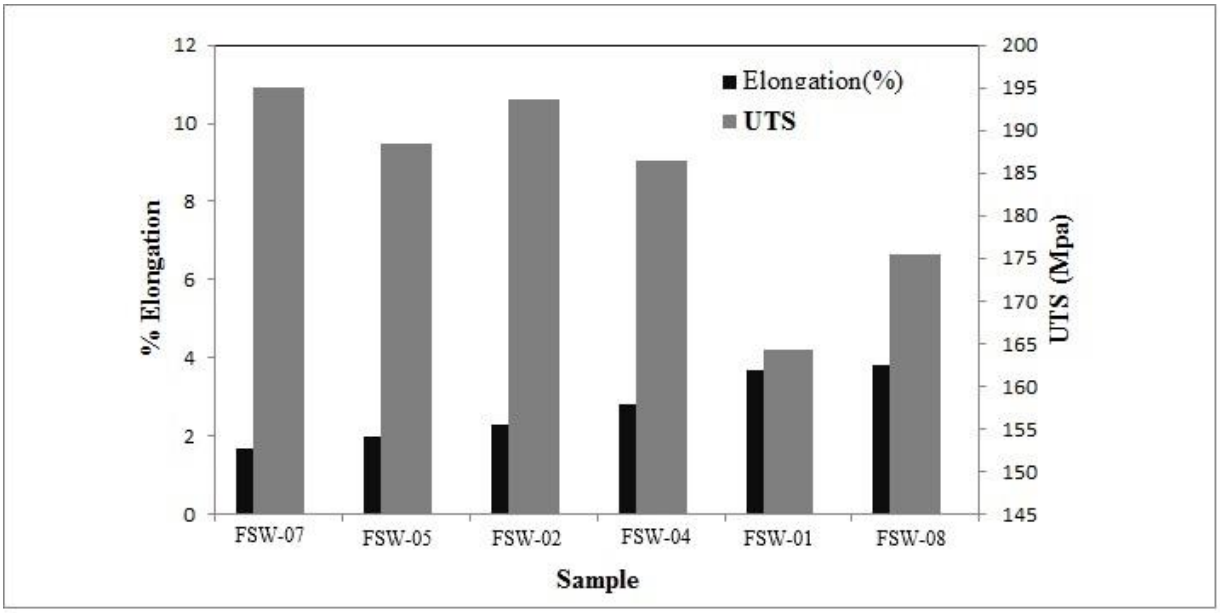

Fig. 6. Elongation and UTS of samples.

Table 5. Mechanical properties of aluminium alloys.

Base Metal	$\sigma_{y(MPa)}$	$\sigma_{UTS\ (MPa)}$	Elongation (%)
2024-T4	268	475	16
7075-T6	442	518	11

It is worth stating that from specimens FSW-01, FSW-02, FSW-04, FSW-05, FSW-07 and FSW-08, specimens FSW-01and FSW-08 were ruled out as non-optimum and unsuitable samples due to their lower ultimate tensile strength. Finally, specimens FSW-02 and FSW-07 were selected as the final optimum specimens due to their higher ultimate tensile strength and off-fusion-zone failure (Table 4).

The microstructure of the welded sheets of the 2024 and 7075 alloys of the optimum welded specimen FSW-02 (1200rpm-70mm/min) is illustrated in Fig. 7. Fig. 7(a) consists of the stir zone (SZ), the HAZ zone (heat-affected zone), and the thermo-mechanically affected zone (TMAZ). Fig. 7(b) only shows the stir zone (SZ). In Fig. 7(a), the 7075 aluminum alloy is on the right side (the successor) and the 2024 aluminum alloy is on the left side (precursor) of the stir zone (SZ). According to Table (4), among the optimum or welding-compatible specimens, in specimens FSW-01, FSW-02, FSW-04, FSW-05, FSW-07 and FSW-08, the stirring number (rotation speed to traverse speed ratio) or the input heat increases with a decrease in the traverse speed at a constant rotation speed. One of the factors influencing the size of the grains in the FSW zone is the mechanical work in the aluminum. With a decrease in the traverse speed the mechanical work increases and more grains are fractured. In this state, the distribution of the grain size is more uniform and wide and it is considered a barrier to the growth of the gains. Recrystallization and mechanical deformation also occur in the stir zone, but at the intersection between the stir zone and the HAZ zone, which is the thermo-mechanically affected zone (TMAZ), less recrystallization occurs and stress-induced deformation is observed.

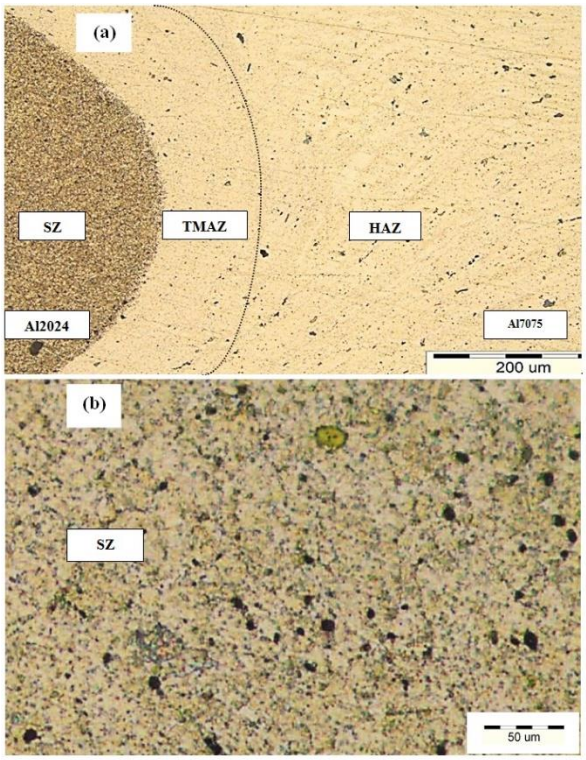

Fig. 7. The microstructure of the specimen FSW-02, (a) low magnification and (b) high magnification.

In the heat-affected zone (HAZ), the recrystallization and extensive deformation occur because the input heat causes a several-millimeter recrystallization around the stir zone (SZ), which results in a considerable structural change. In the specimens with the higher stirring number, the grain size of base metal increases more due to the high input heat.

In the FSW process, a considerable amount of heat is generated, which results in the recrystallization of the grains. The increased heat can be the result of the increased rotation speeds. The material flow from the precursor to the successor, and this transfer goes on around the pin until the material reflows into the precursor. If the plastic material flow is not adequately activated, the adequate amount of materials will not flow into the precursor and the defects in this section will not be repaired. In this research, given the adequate input heat and the suitable rotation and traverse speeds, no hole or defect was observed in the welded aluminum specimens.

The onion rings are concentric semi-circle bands on the cross sections of the FSW specimens. In fact, the onion rings form an eddy and a dynamic re-crystallization zone, where the tip of the tool meets the welding metal. The onion rings form in the stir zone depending on the variations of the different friction stir welding (FSW) parameters [19].

It is worth stating that the onion rings form provided that the adequate input heat and etching are ensured. These parameters result from the adequate traverse and rotation speeds. In general, a smaller stirring number leads to less fluidity and the incomplete formation of the onion rings. On the other hand, a high stirring number (adequate input heat) causes high fluidity as well as the fracture and a mixture of the onion rings [20].

Fig.8 presents the SEM image of the stir zone (SZ) of specimen FSW-10, which has a rotation speed of 1200 rpm and a traverse speed of 70mm/min. In this figure, the light layers are associated with the 2024 alloy, which has a higher copper content than the 7075 alloy. The dark layers also refer to the 7075 alloy, which has a higher zinc content than the 2024 alloy.

The hardness of the 2024-T4 base metal was approximately 135HV and that of the 7075-T6 base metal was app. 170HV. In this research, the hardness of specimens FSW-03, FSW-04, and FSW-09 was measured. These three specimens were selected to identify the changes of hardness at a constant traverse speed and different rotation speed. In all of the specimens, hardness decreased with an increase in the distance from the weld nugget until it reached its minimum level, which identified the interface of TMAZ and HAZ zones. Moreover, the hardness increased to reach the base metal hardness with an increase in the distance from this interface.

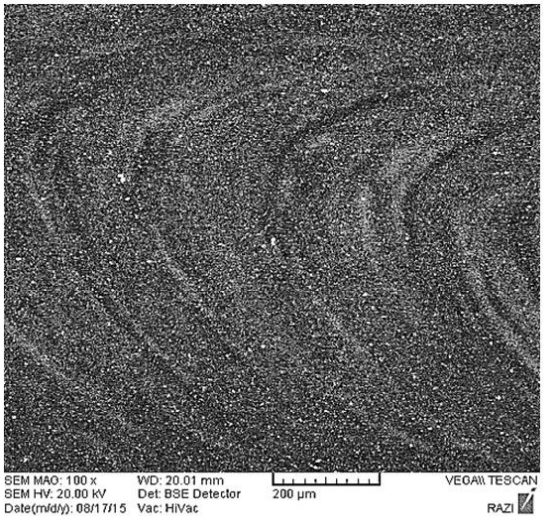

Fig. 8. The SEM image of the stir zone (SZ) of specimen FSW-10.

As seen in Table 4, the highest level of hardness was observed in specimen FSW-04. In addition, as compared to specimen FSW-09, with a decrease in the grain size of FSW-04, the mean hardness of each specimen increased in accordance with the Hall-Petch relation [21]. It is worth stating that the effect of the variation of the rotation speed at a constant traverse speed was examined in specimens FSW-03, FSW-04, and FSW-09 (Fig. 9) by increasing the distance from the SZ zone and using the corresponding hardness profile. In specimens FSW-03, FSW-04, and FSW-09, hardness declined with an increase in the distance from the weld nugget and a decrease in the distance from the weld end. Finally, it was concluded that at a constant traverse speed, with an increase in the rotation speed the stirring number escalated according to Table 4 while the strength and hardness increased. It is worth stating that in all of the hardness profiles, the right side is associated with the 2024 alloy and the left side is associated

with the 7075 alloy. As seen in Fig. 9, the diagram can be split into two asymmetric parts. The 9-mm point is exactly at the center of the diagram in the stir zone. The 7075 alloy is on the left side (dark color) in the SZ zone, and the 2024 alloy is on the right side (brighter color) in the HAZ zone. The highest level of hardness in the fusion zone is associated with the 10-mm point, which is near the 9-mm point in the stir zone and the weld nugget.

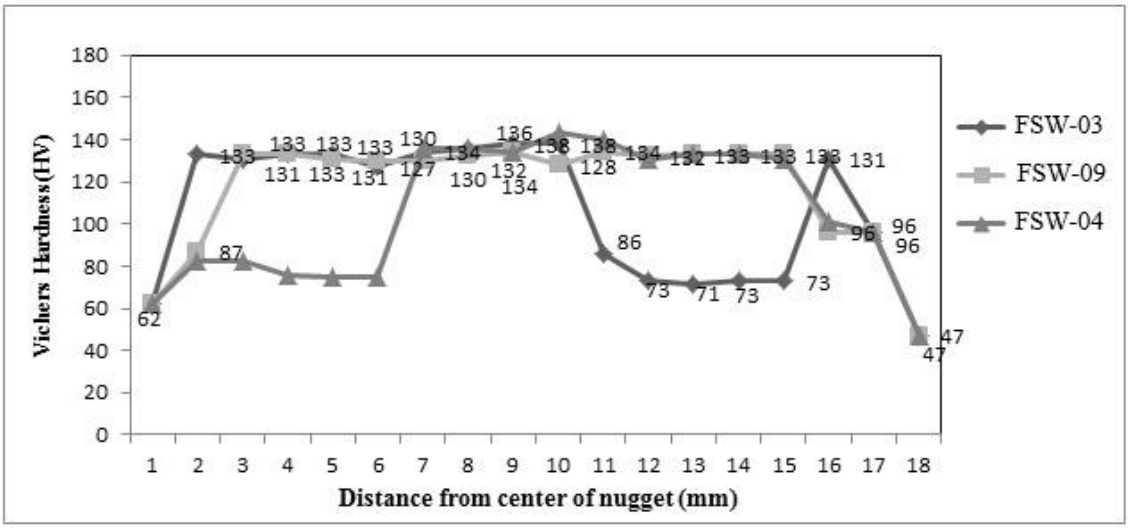

Fig. 9.Hardness value as a function of distance for FSW-03, FSW-04 and FSW-09.

More importantly, as seen in Fig. 9, the difference lies at the center of each side. From the microstructural point of view, this section is almost located on top of the TMAZ zone. Seemingly, with an increase in the rotation speed, the mean hardness profile in the SZ zone increased in the successor or the 7075 alloy or decreased in the precursor side or the 2024 alloy. In other areas, especially the central points, the hardness profiles were almost equal. The ending points on both sides of the diagram show the hardness of the base metals. It is possible to easily compare their hardness to the hardness of the fusion zone. Similar to the research by Bahemmat et al. [22] since these areas contain coarse grains, the hardness of the base metals is lower than the hardness of the fusion zone (FZ), where there are more fine grains. The profile trend on both sides suggests that from the center to the edge of the weld, the trend is almost uniform, and from the edge of the weld to the base metal the mean hardness of the mentioned specimen shows a descending trend.

As stated, the change highlighted in the profiles of specimens FSW-04 and FSW-09 shows that the hardness levels of the two sides of the 9mm point are almost equal and vary in a very small range, reflecting the uniform properties of the weld nugget. According to the hardness profiles illustrated in Fig. 9, in addition to the weld nugget, the highest level of improvement or increase in hardness was observed on the precursor (left) side or the 2024-T4 alloy.

4. Conclusions

The primary goal of this research was to join the 2024-T4 and 7075-T6 aluminum alloys by friction stir welding (FSW) and study the structural and mechanical properties of joint. The following conclusions were drawn from our results:

1) In the process of welding the 2024 and 7075 aluminum alloys, a specimen with a rotation speed of 1200rpm and a traverse speed of 70mm/min and a specimen with a rotation speed of 600rpm and a traverse speed of 30mm/min were selected as the optimum specimens due to their off-fusion-zone failure and high tensile strength

2) The comparison of the specimens in the tensile strength test revealed that with a decrease in the traverse speed, the tensile strength of the specimens increased, the stirring was improved, and the elongation percentage decreased.
3) The highest level of tensile strength (195MPa) obtained under the optimum welding conditions was associated with the specimen with the rotation speed, traverse speed, and elongation percentage of 600rpm, 30mm/min, and 1.7%, respectively.
4) The highest level of hardness in the fusion zone (FZ) was staged by the specimen with the rotation speed of 800rpm, traverse speed of 50mm/min, and hardness of 13808HV. Therefore, this specimen offered a higher level of hardness than the other specimens due to its fine-grained microstructure.

References:

[1] R.S.Mishra,and Z.Y.Ma,"Friction stir welding and processing", Materials Science and Engineering R 50, 2005, pp. 1–78.

[2] Bahemmat P., Rahbari A., Haghpanahi M., Besharati M.K," Experimental Study on the Effect of Rotational Speed and Tool Pin Profile on AA2024 Aluminium Friction stir welded Butt Joints"-*Proceedings of ECTC 2008 ASME Early Career Technical conference* (October 3-4, 2008), Miami, Florida, USA.

[3] D.G. Hattingh, C. Blignault, T.I. van Niekerk, M.N. James, "Characterization of the influences of FSW tool geometry on welding forces and weld tensile strength using an instrumented tool"- *journal of materials processing technology,* Vol. 203 (1-3), 2008, pp. 46-57.

[4] Charit I., Mishra R.S., "Abnormal grain growth in friction stir processed alloys", Scripta Materialia, Vol. 58 (5), 2008, pp. 367-371.

[5] Mohammad Mahdi Moradi, Hamed Jamshidi Aval∗, Roohollah Jamaati, "Effect of pre and post welding heat treatment in SiC-fortified dissimilar AA6061-AA2024 FSW butt joint", Journal of Manufacturing Processes, Vol. 30, 2017, pp. 97–105.

[6] Terry Khaled, Ph.D., "An Outsider Looks at Friction stir welding"-*Chief Scientific / Technical Advisor,* Metallurgy Federal Aviation Administration 3960 Paramount Boulevard. Lakewood, (2005).

[7] D. Ghahremani Moghadam, K. Farhangdost, "Influence of welding parameters on fracture toughness and fatigue crack growth rate in friction stir welded nugget of 2024-T351 aluminum alloy joints", Trans. Nonferrous Met. Soc. China Vol. 26, 2016, pp. 2567−2585.

[8] Akeem Yusuf Adesina∗, Fadi A. Al-Badour, Zuhair M. Gasem, "Wear resistance performance of AlCrN and TiAlN coated H13 tools during friction stir welding of A2124/SiC composite", Journal of Manufacturing Processes 33 (2018) 111–125.

[9] K. N. Krishnan, "The effect of post weld heat treatment on the properties of 6061 friction stir welded joints*", Journal of Materials Science*, Vol. 37(3), 2002, pp. 473–480.

[10] R. Nandan, T. DebRoy and H. K. D. H. Bhadeshia, "Recent Advances in Friction Stir Welding – Process, Weldment Structure and Properties", *Progress in Materials Science,* Vol. 53, 2008, pp. 980-1023.

[11] A. Honarbakhsh-R aouf, H.R. Ghazvinloo and N. Shadfar, " Influence of Friction Stir Welding Variables on Hardness, UTS and Yield Strength of Joints Produced in SSM Cast A356 Aluminum Alloy", *Australian Journal of Basic and Applied Sciences*, Volume 4(8), 2010, *pp.* 3010-3015.

[12] A. Goloborodko, T. Ito, X. Yun, Y. Motohashi and G. Itoh, "Friction Stir Welding of a Commercial 7075-T6 Aluminum Alloy: Grain Refinement, Thermal Stability and Tensile Properties", Materials Transactions, Vol. 45 (8), 2004, pp. 2503 -2508.

[13] Lasley Mark Jason, "*A Finite Element Simulation of Temperature and Materail Flow in Friction stir welding*"-A thesis submitted to the faculty of Brigham Young University in partial fulfillment of the requirements for the degree of Master of Science School of Technology Brigham Young University (April 2005).

[14] Avinash P., "Friction stir welded butt joints of AA2024 T3 and AA7075 T6 aluminum alloys",*Procedia Engineering*,Vol.75,2014, pp.98-102.

[15] A Daneji, M Ali, and S Pervaiz, "Influence of tool geometry and processing parameters on welding defects and mechanical properties for

friction stir welding of 6061 Aluminium alloy", Materials Science and Engineering Vol.346,2018, pp. 1-9.
[16] Kearney, A and Elwin L Rooy. "Aluminum Foundry Products". Edward L. Langer. In Properties and Selection: Nonferrous Alloys and Special-Purpose Material. vol. 2. ASM Handbook. United States of America: ASM International, 1990.
[17] R.S.Mishra,and Z.Y.Ma,"Friction stir welding and processing", *Materials Science and Engineering R*, Vol. 50,2005,pp.1-78.
[18] A. J. Leonard, Friction Stir Welding of Aluminum Alloyes, Proc. 2nd Int. Symp. on Friction stir welding, in TWI, Gothenburg, Sweden, 2009.
[19] A. Scialpi, L.A.C. De Filippis and P. Cavaliere, "Influence of shoulder geometry on microstructure and mechanical properties of friction stir welded 6082 aluminium alloy", Material Design 28 ,2007, pp. 1124-1129.
[20] S. Muthukumaran & S. K. Mukherjee, "Multi-layered metal flow and formation of onion rings in friction stir welds", Int J Adv Manuf Technol Vol. 38, 2008, pp.68–73.
[21] Masaharu Kato, "HallPetch Relationship and Dislocation Model for Deformation of Ultrafine-Grained and Nanocrystalline Metals", Materials Transactions, Vol. 55(1), 2014, pp. 19-24.
[22] P.Bahemmat,M.K Besharati Givi and K.Reshad Seighalani,"The Influence of Welding Speed on Microhardness and Microstructure in Dissimilar Friction Stir Welded of AA6061-T6 and AA7071-T6", *The International Institue of Welding(IIW)Congress Welding & Joining*,pp.397-402,2009.